6-22-2023

Reduction of Inter-aquifer Water Exchange by Sand-Bentonite mixture

Angel Jimenez

REDUCTION OF INTER-AQUIFER WATER EXCHANGE BY SAND-BENTONITE MIXTURE

by

Angel Alberto Jimenez Leon

A Dissertation

Submitted in Partial Fulfillment of the

Requirements for the Degree of

Doctor of Philosophy

Major: Civil Engineering

University of Memphis

May 2023

DEDICATION

To my father in heaven, to my mother, to Sonia, my wife, and to my children Patrisia, Andrea, Paola y Juan Alberto and to my grandchildren Florence, Charlotte, Enzo, Lucas Alberto, and Elsie.

ACKNOWLEDGMENTS

My imperishable thanks to Dr. Brian Waldron for all the support provided during the completion of this dissertation, his help has been essential to successfully completing this academic degree. I also want to express my gratitude to all members of the Committee who contributed with their knowledge and expertise to this manuscript. I also expressly wish to acknowledge the help provided during the completion of this dissertation to The University of Memphis and the Center for Applied Earth Science and Engineering Research (CAESER), especially to Dr. Daniel Larsen, Dr. Scott Schoefernacker, Dr. Farhad Jazaei, and Rodrigo Villalpando-Vizcaino. The help of this center was fundamental in the culmination of this work. I would also like to thank Memphis Light, Gas and Water (MLGW) for the funding support provided for this project.

Thank you to all my family, especially to my wife and to my children and grandchildren, whose unconditional support was invaluable to succeed in the achievement of this degree.

PREFACE

This work is formatted in the style of the *Journal of Environmental Engineering*, to which it will be submitted for publication.

ABSTRACT

A confined to semi-confined water-supply aquifer beneath Memphis, the Memphis aquifer is protected in most areas by an upper natural hydraulic barrier referred to as the upper Claiborne confining unit (UCCU), which acts as an aquitard and is mainly comprised of clay and silt. Studies of the UCCU have revealed breaches, which allow cross-contamination or inter-aquifer exchange of water between the unconfined (shallow) and the underlying Memphis aquifers. This study examines the possibility of filling the voids within a preferential pathway in the UCCU via sand-bentonite mixture to reduce the inter-aquifer exchange between the shallow and Memphis aquifers.

The research examined the development of a sand-bentonite mixture whereby the voids of the coarse particles of the sand are filled out by adding certain percentages of small-sized particles of bentonite to arrive at a maximum or optimal mixing ratio. Two types of parent media were used in the laboratory experiments: fine, medium, and coarse glass beads; and sand extracted from a core through a known breach in the UCCU. Hydraulic conductivity was measured in 76 samples prepared with a range of bentonite from 0%, 10%, 20%, 25%, and 30%, and the flow conditions were modeled in an idealized conceptual model using MODFLOW to assess the reduction of the flux resulting from the experimentally determined ideal sand-bentonite mixtures.

The experimental results show that the hydraulic conductivity is reduced by two orders of magnitude in the coarse glass beads, four orders of magnitude in the medium glass beads, and achieves the same order of magnitude of a UCCU-type clay conductivity at 6% bentonite for the fine glass beads and the sand, reaching a 2-order of magnitude further decrease at 10%

bentonite (4.22 x 10^{-6} m/day). Modeling showed that the vertical flux (q) reached at 6% bentonite approximated the flux through the UCCU clay. As bentonite percentages increased toward 10%, the flux reduced to 0.06 m/day, plateauing thereafter over differing injection thicknesses (0.5-5 m).

TABLE OF CONTENTS

Chapter Page

List of Tables **Page**

.

List of Figures **Page**

INTRODUCTION

Contamination of groundwater in a multi-layer system threatens its sustainable use (Ryan et al., 2022) and is thus an imperative problem to resolve (Carmichael et al., 2018; Qian et al., 2020). Aquitards provide protection from contamination to confined aquifers by impeding or preventing the movement of groundwater from water-table (shallow) aquifers to the underlying confined aquifers (Rine et al., 2004; Santi et al., 2006). Unfortunately, there are routes through which groundwater contamination may still result: inter-aquifer water exchange due to aquitard leakage (Villalpando-Vizcaino et al., 2021); localized discontinuation within a low-permeability aquitard (here termed breaches) (Santi et al., 2006), or through water pumping from the confined aquifer (Jiménez-Martínez et al., 2011) where exchange results from faults, poor annular seals along a well, or other mechanisms. The construction of barrier systems, also called hydraulic barriers (Takai et al., 2013), has long been used to control, reduce, or eliminate aquifer contamination (Pearlman, 1999; Takai et al., 2016). Common methods of installing hydraulic barriers include the use of mixtures (Alkaya and Esener, 2011; Evans et al., 2020), the growth of microorganisms (Seki et al., 1996), and vitrification (Tixier & Thompson, 1993; Oma, 1994; Li & Zhang, 2013; Staley, 1995; Trifunović, 2021;).

The hydraulic, nonstructural, and subsurface vertical and horizontal barriers (Ryan, 1985; Pearlman, 1999; Takai et al., 2013) use a mixture of coarse and fine materials (Pearlman, 1999) where the ratio of the diameter of coarse materials to the diameter of fine materials should be 6.5 to 1, as defined in Table 1 (Cubrinovski & Ishihara, 2002). Less common techniques for controlling groundwater flow involve vitrification and the growth of microorganisms. Vitrification involves the use of in-situ and ex-situ thermal technology (Tixier & Thompson, 1993; Staley, 1995; Trifunović, 2021), where the amorphous material is heated

to high temperatures ranging from 1,400 to 7,000 degrees Celsius then rapidly cooled so the molecules are not able to form crystalline structures but instead transform the material into a glassy solid barrier (Li & Zhang, 2013; Trifunović, 2021). The vitrification method is limited to an area of approximately 12 x 12 meters, a maximum depth of about 6 meters, and 1,000,000 kg total mass with the in-situ vitrification (ISV) technology (Oma, 1994; Li & Zhang, 2013). In the microbial method, microorganisms are used to fill voids in the soil with gases produced by anaerobic substances (Seki et al., 1996).

Vertical barriers, also referred to as cutoff walls (Ryan, 1985; Xu et al., 2016), are used to prevent the horizontal flow of groundwater or contaminants (Ryan & Day, 2002; Takai et al., 2016). Vertical barriers are more commonly used than horizontal barriers (Karp et al., 1962); however, they cannot control the downward migration of contaminants that fall within their boundaries (Durmusoglu & Corapcioglu, 2000). There is abundant information on the construction and design of vertical barriers (Anderson & Mesa, 2006) with four main types of barrier installation methods (Evans et al., 2020): (1) soil-bentonite (SB) slurry trenches, which is the most sustainable method; (2) self-hardening slurry trenches of cement-bentonite or slag-cement-bentonite (CB); (3) soil mixed wells (SM); and (4) sheet pile walls (SP). Horizontal barriers are used to prevent the vertical flow of groundwater (Durmusoglu & Corapcioglu, 2000) and are typically used as horizontal liners in landfills (Ojuri & Oluwatuyi, 2017). Horizontal barriers also prevent seepage between wet and dry surfaces at nuclear waste repositories (Srikanth & Mishra, 2016); however, these barriers have not been studied in detail regarding limiting inter-aquifer water exchange. Since vertical barriers cannot control downward migration, the use of horizontal barriers is becoming more common through directional drilling in environmental projects (Durmusoglu & Corapcioglu, 2000).

Soil-bentonite mixtures have been used for the past 70 years to control groundwater flow (Ryan, 1985; Ryan & Day, 2002; Ryan et al., 2022; Koch, 2002) and in many

environmental, civil and geotechnical works (Ryan, 1985; Koch 2002; Castelbaum & Shackelford, 2009; Alkaya & Esener, 2011; Sun et al., 2015; Takai et al., 2016; Srikanth & Mishra, 2016; Ojuri & Oluwatuyi, 2017; Yin et al., 2021) . Voids between sand particles are filled by a percentage of bentonite particles, providing a low hydraulic conductivity barrier to flow (Takai et al., 2013; Hwang et al., 2011; Alakayleh et al., 2018). Bentonite is known for swelling more than most other clays, reducing the amount required for the mixture (Sivapullaiah et al., 2000; Alkaya & Esener, 2011; Ghazi, 2015; Sun et al., 2015; Ojuri & Oluwatuyi, 2017), as well as for its exceptional physical, structural and chemical properties (Koch, 2002; Wang et al., 2012; Ryan et al., 2022).

A wide range of laboratory studies have examined various performance aspects of the sand-bentonite mixture including determining its hydraulic conductivity based on an optimal mixing ratio (Seki et al., 1996; Sällfors & Öberg-Högsta, 2002; Zhang et al., 2009; Xu et al., 2016), minimum and maximum void ratios (Cubrinovski & Ishihara, 2002; Othman & Marto, 2018), effects of particle sizes (Srikanth & Mishra, 2016), and soil-structure interface (Yin et al., 2021). However, these studies are limited to sand-bentonite mixtures that are used as liners in either waste disposal (Sällfors & Öberg-Högsta, 2002; Srikanth & Mishra, 2016), water retention (Sivapullaiah et al., 2000), or nuclear waste (Sun et al., 2015).

The Memphis aquifer is a semi-confined unconsolidated sand aquifer located beneath Memphis, Tennessee, and is part of the multi-state Mississippi embayment aquifer system (Parks, 1990; Waldron et al., 2009). This aquifer is mostly protected by the overlying upper Claiborne confining unit (UCCU), which is primarily composed of clay and silt that limit groundwater flow to the Memphis aquifer from the overlying shallow aquifer (Carmichael et al., 2018). Local studies on the UCCU have revealed preferential pathways, termed “breaches”, that allow water of poorer quality from the shallow aquifer to enter the Memphis aquifer due to a downward vertical gradient caused by extensive pumping in the Memphis aquifer (Parks,

1990; Bradley, 1991; Parks et al., 1995; Larsen et al., 2003; Waldron et al., 2009; Smith, 2018; Carmichael, et al., 2018).

The present study examines the development of a sand-bentonite mixture for application to horizontal barrier whereby the voids of the coarse particles of the sand are filled in by adding certain percentages of small-sized particles of bentonite to arrive at a maximum or optimal mixing ratio (Cubrinovski & Ishihara, 2002; Chung et al., 2018). No previous studies are known to examine the possibility of reducing the inter-aquifer exchange between the shallow and Memphis aquifers by installing a horizontal hydraulic barrier in the UCCC using a sand-bentonite mixture. Laboratory experiments were conducted using two types of parent media: small, medium and coarse glass beads (Riha et al., 2018), and sand extracted from a known breach in the UCCU obtained through sonic drilling. Hydraulic conductivity was measured in 76 samples prepared with the addition of 0%, 10%, 20%, 25%, and 30% bentonite by mass (Hwang et al., 2011; Ghazi, 2015; Takai et al., 2016; Srikanth & Mishra, 2016; Chung et al., 2018; Sakita et al., 2020).

MATERIALS AND METHODS

Laboratory experiments were conducted to find the optimal mixing ratio in the sand-bentonite mixture. Table 1 summarizes relevant data for each of the materials used: Coarse glass beads (CGB), medium glass beads (MGB), fine glass beads (FGB), bentonite (B), and sand (SA) extracted from within an aquitard breach borehole core (99s2). Saturated hydraulic conductivity (K) was measured for each mixture only until 30%, using standard procedures to determine the optimal mixing ratio for each mixture (Chung et al., 2018)

Table 2. Mixtures of coarse and fine materials.

Mixtures	Type of Coarse Material	Grain Diameter (mm)	Type of Fine Material	% of Sodium Bentonite
CGB + 10, 20, 25, 30 40 % B	Coarse Glass Beads (CGB)	0.8-1.1	Sodium Bentonite (B)	10-20-25-30-40
MGB + 10, 20, 25, 30, 40 % B	Medium Glass Beads (MGB)	0.545-0.841		
FGB + 10, 20, 25, 30, 40 % B	Fine Glass Beads (FGB)	0.125-0.25		
SA + 10, 20, 25, 30, 40 % B	Sand from borehole 99s2 (SA)	0.125-0.4		

TESTING MATERIALS

Glass beads

Glass beads of different sizes were utilized because of their uniformity and ability to provide a homogenous environment that would avoid difficulties from using real sand

(Syngouna & Chrysikopoulos, 2015). The beads used are as follows: coarse grade smooth glass beads (0.8 to 1.1 mm); medium grade smooth glass beads (0.545 to 0.841 mm); and fine grade smooth glass beads (0.125 to 0.25 mm).

Sand

The sand utilized in the experiments was obtained through sonic drilling from borehole 99s2 from a known breach in the UCCU. The UCCU breach is approximately 65 m thick. A composite sample of the sand was obtained from the top (16.5 m), middle (49.0 m), and bottom (82.0 m) depths of the breach. Since our goal was to reduce the hydraulic conductivity (K) of the breach by at least five orders, assessing our methodology on sand from within a breach was critical.

Bentonite

Sodium bentonite was used as the fine material in laboratory experiments. It is a premium-grade, high-yielding Wyoming sodium bentonite with particles range from 0.1 pm to 44 pm. This sodium-bentonite is a highly plastic clay (categorized by ASTM, 2011) with a specific gravity of 1.59 (g/cm^3) (Chegbeleh et al., 2009). Bentonite's high capacity to swell, high water absorption, low hydraulic conductivity, and its self-sealing characteristic made it a viable choice to fill voids in the sand porous media (Alzamel M.et al., 2022).

EXPERIMENTAL PROCEDURE

Property Measurements of the Materials and Mixtures

The most important property of the materials and the mixtures formed from them is the void ratio, which is the ratio of the volume of voids to the volume of solids. The void ratio depends in part on the material's grain size distribution and in a porous media can be filled with material

of differing grain sizes (Cubrinovski & Ishihara, 2002). Voids in sand are influenced by percent fines, grain-size composition and shape, and packing arrangement (Cubrinovski & Ishihara, 2002). Maximum void ratios (e_{max}) and minimum void ratios (e_{min}) in a mixture are dependent on the fine content of the soil (Chang et al., 2016). When fines are added to sand, the void ratio is reduced due to (1) filling the voids, then (2) replacing the solids (Cubrinovski & Ishihara, 2002). Several properties of mixtures (defined in Table 1) were measured in the laboratory, including bulk density, dry density, particle density, void ratio, and porosity.

Hydraulic Conductivity Test

Laboratory experiments were conducted to determine the hydraulic conductivity of the glass bead and sand samples with various clay percentages. Following a design concept by Cubrinobski et al. (2002), increasing percentages of fine material (i.e., bentonite) were added to glass bead groups of fine, medium and coarse based on their diameter to ascertain measures of hydraulic conductivity and to observe when values drastically reduced to approximate a clay barrier. ASTM D5084-16a was followed using method B of Chung et al. (2018). Of note, this method includes compaction of the material by adding a sequence of layers with hand compaction, scarifying each layer before the next layer was applied according to ASTM D5084-16a. Compaction is appropriate when considering that the sand samples were originally under 16.5 m of overburden material.

Sample Preparation

Each test specimen (glass beads and sand) was prepared by mixing 10, 20, 25, 30, and 40% of dry powder sodium bentonite per dry weight of the mixture. To calculate the mass of

dry bentonite (m_B) to add, a measure was made using Equation (1) (Li et al., 2021) where the mass of the parent material (sand or glass) was known and %bentonite (P_B) stipulated.

$$m_B = \frac{P_B m_S}{(100 - P_B)}\ ,\ kg \qquad (1)$$

where:

m_B- mass of sodium bentonite, kg.

P_B- percentage of bentonite, %.

m_S- mass of sand material, kg.

Sample preparation occurred in a DGSI-S-480 permeability cell, using the DGSI-S-500 permeability panel, a split vacuum mold, and a latex membrane. Each test specimen was set to 0.071 m in diameter and 0.15 m in height. Following the DGSI setup procedure, the latex membrane was first assembled in the base pedestal of the permeability cell and fixed with two O-rings. A porous stone was then introduced, and the split vacuum mold was adjusted to the base of the permeability cell. The split mold was then vacuumed to conform the latex membrane to the mold. The desired mixture was then added to the mold in layers that were leveled after each layer addition, then compacted following ASTM D5084-16a. Lastly, the split mold apparatus was placed within the permeability panel and vacuumed again before removing the split mold.

Measurement of Hydraulic Conductivity

This study focuses on the determination of sand-bentonite mixtures that fill the voids between parent particles with bentonite but do not displace the particles. Additionally,

achieving full saturation of the samples was important (Bárcena & Hurtado, 1999); therefore, water was used to confine the sample in the testing chamber to 21 kPa while maintaining zero pore pressure in the sample. A back pressure was applied to the sample in increments of 35 kPa up to 345 kPa while also incrementally increasing the cell pressure to 35 kPa from its starting pressure of 21 kPa. A Skempton B coefficient was calculated for each sample to ensure saturation was achieved where coefficients should be between 0.95 and 1.0 (see Table 4) (Bárcena et al., 1999). To determine glass bead diameters, grain size analysis of the same breach sand used in this experiment was analyzed by Hasan (unpublished). It is recognized that aquifer sands vary in coarseness from coarse to fine. Hasan (unpublished) determined that 89% of the aquitard breach sand particles were characterized as fine (Figure 1); therefore, the fine glass bead diameter was approximated from this and medium and coarse from U.S. Department of Agriculture Soil Classification System.

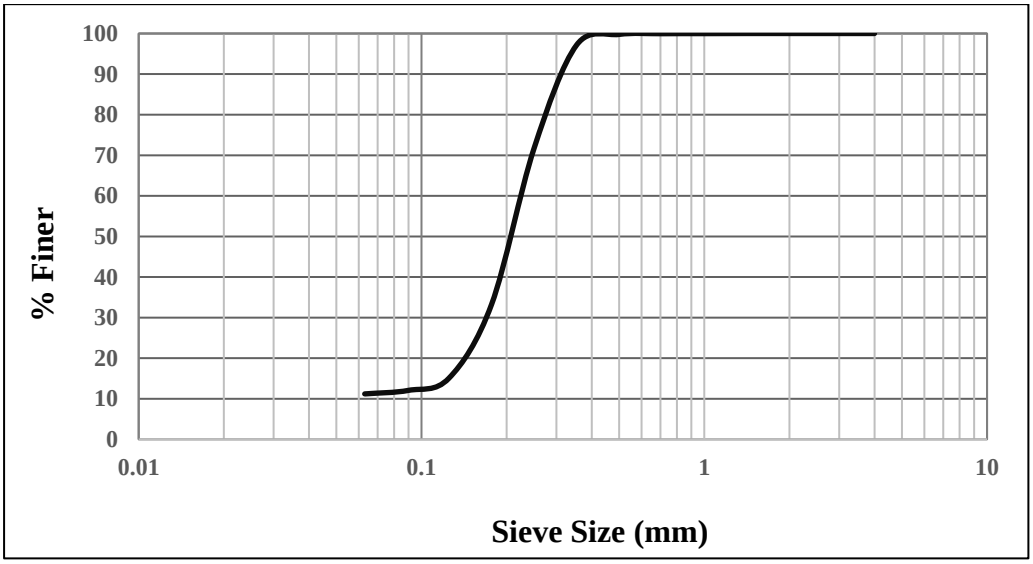

Figure 1. Sieve analysis of SA (Hasan K., unpublished).

Hydraulic conductivity was measured using a permeability cell DGSI S-480 and BK panel S-500. Prior to determining hydraulic conductivities of the mixtures (i.e., parent material + bentonite), measure of hydraulic conductivities (K) of coarse, medium and fine glass beads

were compared to published values (Riha, 2018). This not only ensured adherence to ASTM procedures, but that the instrument was working properly as it required maintenance prior to the experiments. Upon verification, hydraulic conductivity experiments were conducted on glass bead-bentonite composite sand-bentonite mixtures. Vertical hydraulic gradients ranged between 2 and 15 based on some preliminary tests. Hydraulic conductivity was calculated using Equation (3) for falling-head tests with constant tailwater pressure (ASTM, 2016):

$$K = \frac{a.L}{A.\Delta t}\ln\left(\frac{h_1}{h_2}\right) \quad (3)$$

where:

K = hydraulic conductivity, m/s.

a = cross-sectional area of standpipe, m^2.

L= length of mixture specimen, m.

A= cross-sectional area of mixture specimen, m^2.

Δt= interval of time, s.

h_1= initial reading of head loss across the permeameter at t_o, m.

h_2= final reading head loss across the permeameter at $t_o + \Delta t$, m.

The value of hydraulic conductivity was taken after three consecutive measurements fell within 10% of the mean value (Dai et al., 2020). Lastly, the hydraulic conductivity was corrected to a standard temperature of 20 ^oC using measured sample temperatures taken during each experiment following ASTM D5084-16a.

DEVELOPMENT OF A NUMERICAL MODEL

A field test of injection was not possible with this investigation; however, a determination of its application can be performed using a conceptualization of an aquitard

breach that includes variables obtained from other studies and the hydraulic conductivity ranges developed from this study. The conceptual model included a multi-layered aquifer system comprised of an unconfined aquifer, an aquitard, and a deeper, confined aquifer with three pumping wells at various depths to simulate a small wellfield. A breach is implied through the aquitard to make a more permeable hydraulic connection between the aquifers. The gradient of flow is from the shallow aquifer to the confined aquifer, thus downward through the breach.

The model used the pre- and post-processing software Groundwater Modeling System (GMS v.10.6 by Aquaveo) and was discretized into a MODFLOW-2005 (Harbaugh, 2005) finite-difference 3D grid with 250,000 cells based on 50 rows, 50 columns, and 100 layers. The cells had a uniform horizontal dimension of 10 m with a thickness of 0.5 m. Sequencing from top to bottom, the unconfined aquifer represents the upper 30 layers, the aquitard the next 30 layers and the confined aquifer the bottom 40 layers. The aquitard breach was simulated as a 10 x 10 cell area within the aquitard that extended entirely through its 30 layers.

Three main scenarios were assessed: non-leaky aquitard, aquitard breach with hydraulic parameters from real sand, and aquitard breach with different bentonite percentages (0 to 10%). Each scenario was assessed using different layer thicknesses of 0.5 m, 1.0 m, 2.0 m, and 5.0 m to determine the influence of injection thickness on inter-aquifer exchange. The mechanics of injection and behavior of void closure (i.e., filling of the voids) were not modeled; instead, proper injection that homogenously filled the entire layer was assumed.

In general, bentonite slurries have exceptional engineering properties (Yoo et al., 2006) such as physical, structural, and chemical properties (Koch, 2002; Wang et al., 2012; C. Ryan et al., 2022). They are used for several purposes such as tunnel excavation (Lei et al., 2022), mechanized tunneling (T. Xu et al., 2017), slurry cutoff walls (C. R. Ryan, 1985), improving sand strength by filling the voids between sand particles (Bani Baker et al., 2022), strength and

reduction of swelling soils (Sharo et al., 2022), stabilization of sandy soils (Bani Baker et al., 2022), and improvement of sintering, adhesive strength, corrosion, and resistance to alkali of injection repair mix (Z. Li & Dou, 2008).

Slurry injections have their share of challenges (Veil & Dusseault, 2003; Namil & Gular, 2019). Slurry viscosity is one such factor where additives to improve its viscosity have included polyvinyl alcohol (Dai et al., 2020) and ethanol alcohol (Chegbeleh et al., 2009; Takase et al., 2011), although any harm produced by using these additives should be considered. Other factors to consider are the type of parent material being injected into (Holmboe et al., 2011), chemical compatibility (Q. Li et al., 2021), and electrical conductivity (Yoo et al., 2006).

RESULTS AND DISCUSSIONS

MEASUREMENTS OF THE PROPERTIES OF THE MATERIALS AND MIXTURES

As can be seen for all samples, the bulk density, void ratio (e_{min}) and porosity, values increase with increasing bentonite until reaching a threshold bentonite content where the trend reverses. For example, for MGB, bulk density increases gradually from 1812.,62 kg/m^3 at 0% bentonite to 2050.65 kg/m^3 at 25% bentonite before declining to 1962.63 kg/m^3 at 40%. Bentonite and porosity follow a similar change in trend at the same bentonite contents.

Table 2. Properties of the materials and their mixtures. Note: mixture characterization at 40% bentonite is provided but was not used in the experiments.

Material	Bentonite, %	Bulk density, (kg/m^3)	Particle density, (kg/cm^3)	Void Ratio, e $_{min}$	Porosity, (%)
CGB	0	1.85E+03	2.53E+03	0.535	34.9
	10	1.93E+03	2.61E+03	0.440	30.6
	20	2.05E+03	2.75E+03	0.391	28.1
	25	2.11E+03	2.84E+03	0.381	27.6
	30	2.14E+03	2.95E+03	0.378	27.4
	40	2.10E+03	3.28E+03	0.422	29.7
MGB	0	1.81E+03	2.54E+03	0.533	34.8
	10	1.89E+03	2.58E+03	0.413	29.2
	20	2.01E+03	2.72E+03	0.369	26.9
	25	2.05E+03	2.83E+03	0.365	26.8
	30	2.01E+03	2.96E+03	0.372	27.1
	40	1.96E+03	3.27E+03	0.411	29.1
FGB	0	1.68E+03	2.56E+03	0.533	34.8
	10	1.86E+03	2.58E+03	0.338	25.2
	20	1.83E+03	2.82E+03	0.339	25.3
	25	1.81E+03	2.95E+03	0.347	25.8
	30	1.79E+03	3.10E+03	0.361	26.5
	40	1.75E+03	3.44E+03	0.402	28.7
SA	0	1.51E+03	2.42E+03	0.487	32.7
	10	1.72E+03	2.47E+03	0.238	19.2
	20	1.68E+03	2.78E+03	0.273	21.5
	25	1.64E+03	2.93E+03	0.290	22.5
	30	1.60E+03	3.10E+03	0.314	23.9
	40	1.53E+03	3.48E+03	0.368	26.9

Using e_{min} to explain, Figures 2, 3, 4 and 5 indicate that at the point of trend shift, any further addition of bentonite begins to "replace" the parent material. Recall that the purpose of this experiment is to replace voids with bentonite assuming a fixed volume. When excessive bentonite percentages were added, the volume of the sample essentially increased, though only to a minor extent, but enough to be indicated in the trend shifts observed in Table 2 whereby e_{min} was exceeded (past the trend shift point). Hence, Figures 2, 3, 4 and 5 indicate the optimum bentonite percentage for CGB, MGB, FGB, and SA as 30%, 25%, 10%, and 10%, respectively.

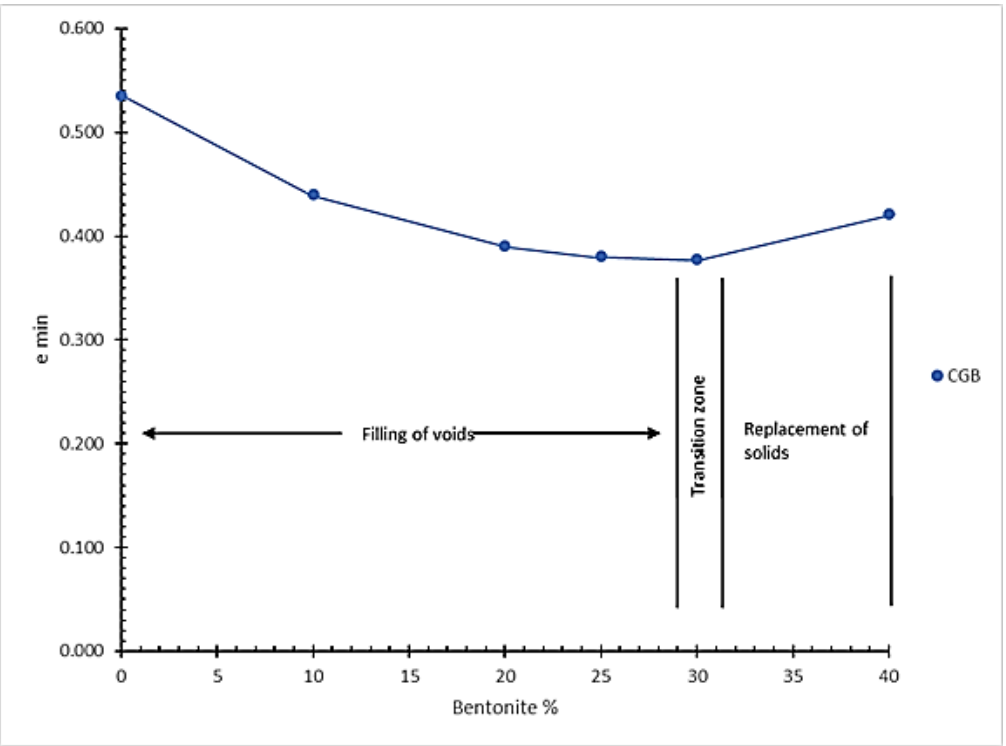

Figure 2. Void ratio for CGB

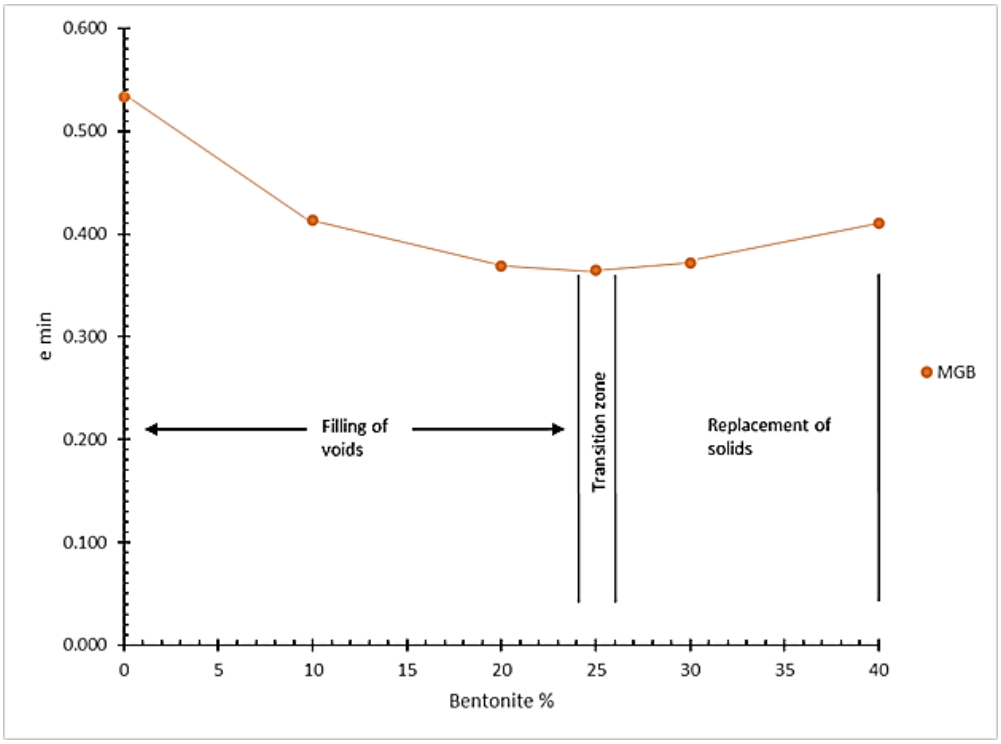

Figure 3. Void ratio for MGB

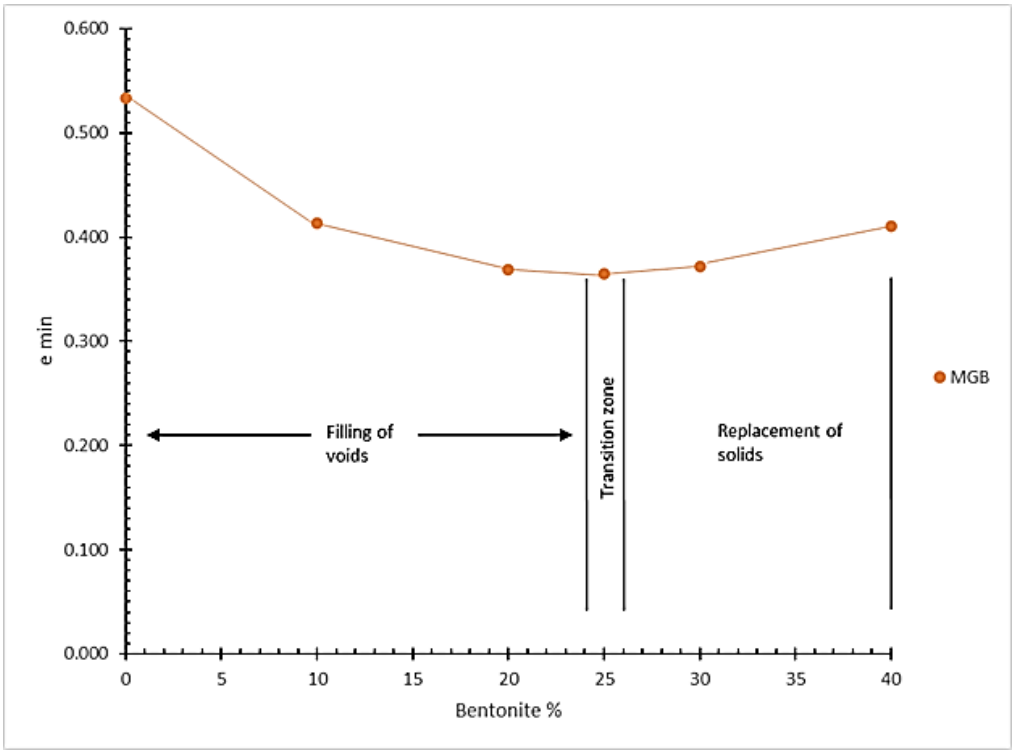

Figure 4. Void ratio for FGB

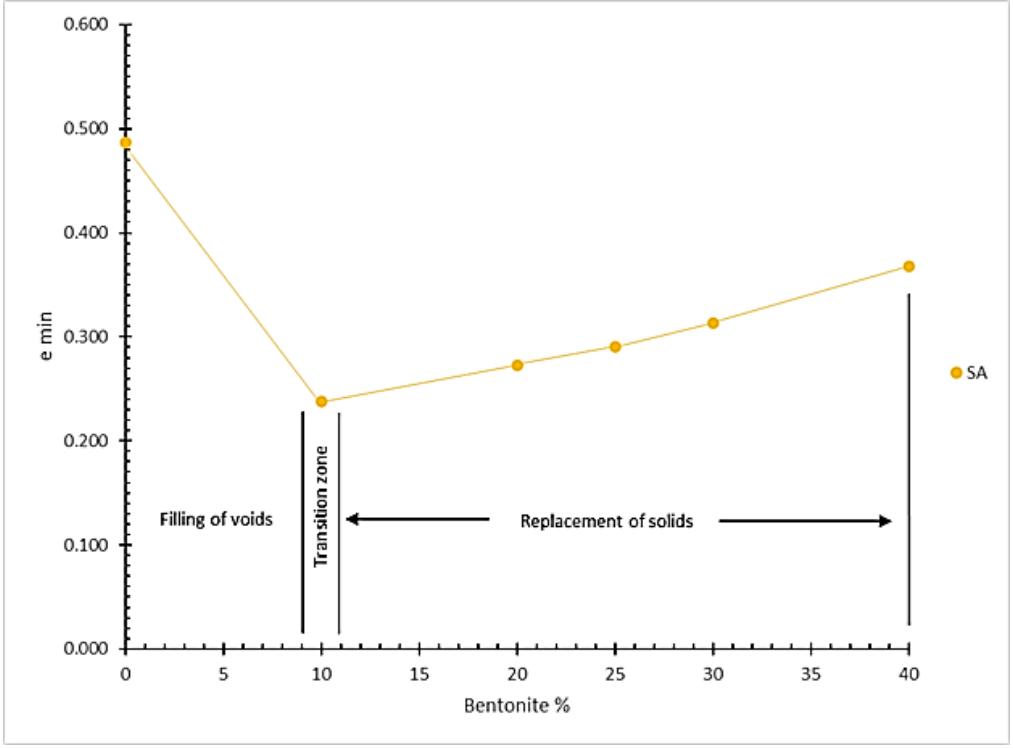

Figure 5. Void ratio for SA

COMPARISON OF HYDRAULIC CONDUCTIVITY: PUBLISHED VS. EXPERIMENTAL

Initial experiments were conducted on the glass beads to compare lab-derived hydraulic conductivity (K), using ASTM D5084-16a, with published values by Riha et al. (2018), as shown in Table 3. As the diameters of our fine and medium glass beads did not match those by Riha et al. (2018), a relationship for K_{min} and K_{max} was developed (Figure 6) and predicted values of K's derived from the fitted equations.

Table 3. Predicted Hydraulic conductivity based on the diameter of glass beads.

Type of GB	Published (Riha, 2018)			Experiment Diameter (mm)	Predicted (Riha, 2018)		K measured	
	Diameter (mm)	Kmin (m/day)	K max (m/day)		K min (m/day)	K max (m/day)	Kmin m/day	Kmax m/day
FGB	0.1750	11.23	31.10	0.1875	12.92	33.17	13.3	37.1
MGB	0.4950	95.04	190.08	0.6930	189.13	399.11	399	403
CGB	0.9500	359.42	796.61	0.9500	359.42	796.61	797	807

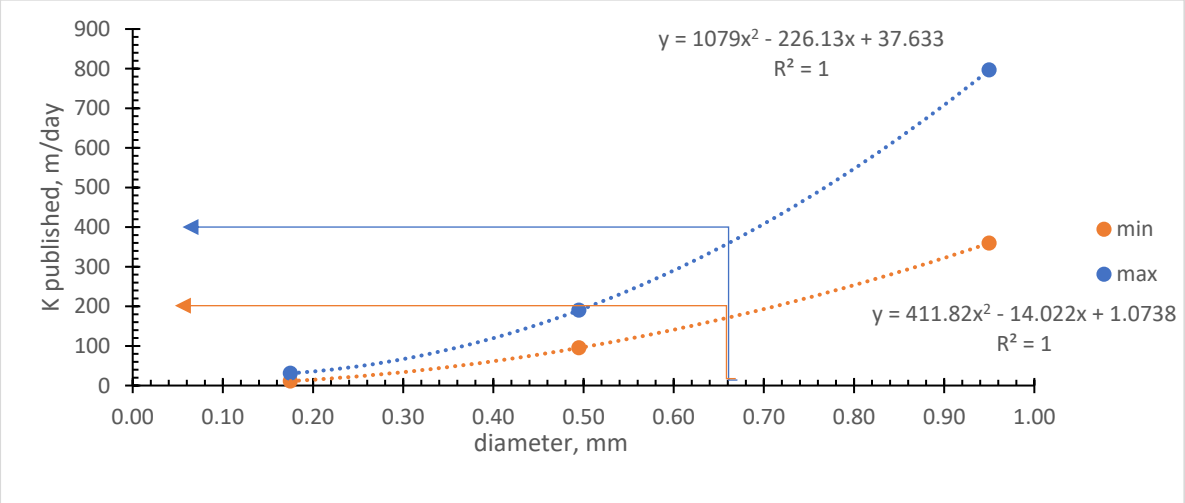

Figure 6. K published vs diameter of glass beads (CGB, MGB, FGB). Blue and orange arrows indicate the extraction of K_{min} and K_{max} for MGB, as an example.

Hydraulic conductivity measurements were then obtained for FGB, MGB and CGB where a K_{min} and K_{max} were extracted from multiple experiments (Table 3). Experimental K_{min}'s were higher than predicted, ranging between 0.68 and 2.55% higher. Similarly, experimental K_{max}'s were also higher than predicted values but with a larger range of 1.04 to 11.97%. Higher differences for K_{min} and K_{max} both occurred for FGB due to difference in the size of particle diameters. Differences may be explained by the compaction method. Published K's represent a compaction by vibration versus our hand compaction, where the prior creates a tighter packing thus resulting in lower K values. However, the match between published values and our experimental K's was considered strong because for K_{min} had a very strong positive correlation coefficient (R=0.999), an adjusted coefficient of determination of R^2=0.999, and a standard error of 2.13. K_{max} was similar to K_{min} except for having a standard error of 2.50.

LAB EXPERIMENTS ADDING BENTONITE

Bentonite was added to each glass bead type at increments of 10, 20, 25, and 30% and to the aquitard breach composite sand sample (SA) at 5% increments from 0-10%, then at 20, 25, and 30%. A bentonite additive of 30% was the maximum amount before transitioning to replacement of the parent material (see Figures 2 and 3); however, for FGB and SA the optimum bentonite addition was 10% (Figures 4 and 5). Experiments with FGB and SA above 10% bentonite were included for comparison with CGB and MGB, knowing that the threshold to replacing particles was surpassed; however, there was still no significant gain in the average hydraulic conductivity.

As shown in Table 4, K_{avg} for CGB shows a 2-order of magnitude reduction to 1.13 m/day at 30% bentonite. A 4-order of magnitude reduction in K_{avg} occurs for MGB achieving a low of 3.98×10^{-2} m/day. FGB achieved at 10% bentonite a K_{avg} (1.12×10^{-4} m/day) approximating UCCU clay conductivities reported by Villalpando et al (2021) at 5.7×10^{-4} m/day. Within the same order of magnitude, a UCCU-type clay conductivity was obtained at 6% bentonite for SA, reaching a 2-order of magnitude further decrease at 10% bentonite (4.22×10^{-6} m/day). Robinson et al. (1997) reported UCCU hydraulic conductivity ranging between 3.0×10^{-4} to 1.5×10^{-6} m/day. Clark and Hart (2009) use a hydraulic conductivity of 4.7×10^{-2} m/day to represent the UCCU in a numerical model; however, this single value represented the UCCU covering portions of six states. For % bentonite exceeding 10% for FGB and SA, the hydraulic conductivity did not notably change.

Table 4. Hydraulic conductivity for bentonite mixtures. Red numbers indicate an average hydraulic conductivity representative of the UCCU clay (Villalpando et al. 2021; Robinson et al. 1997)

Type of material	**Na-Bentonite** %	**K max** m/day	**K min** m/day	**K average** m/day	**B-Skempton Coefficient**
Coarse glass beads (CGB)	0	8.07E+02	3.62E+02	5.85E+02	1
	10	4.07E+02	8.87E+01	2.48E+02	0.98
	20	1.51E+02	3.60E+01	9.35E+01	0.95
	25	3.77E+01	7.08E+00	2.24E+01	0.95
	30	2.19E+00	6.17E-02	1.13E+00	0.95
Medium glass beads (MGB)	0	4.03E+02	1.93E+02	2.98E+02	1
	10	6.21E+01	4.36E+01	5.28E+01	0.97
	20	1.11E+01	7.43E-01	5.93E+00	0.98
	25	4.62E-02	5.46E-03	2.58E-02	0.96
	30	7.12E-02	8.42E-03	3.98E-02	0.95
Fine glass beads (FGB)	0	3.71E+01	1.32E+01	2.52E+01	1
	10	1.67E-04	5.72E-05	1.12E-04	0.96
	20	1.69E-04	5.84E-05	1.14E-04	0.95
	25	1.70E-04	5.89E-05	1.15E-04	0.95
	30	1.72E-04	5.91E-05	1.16E-04	0.95
Sand from 99s2 (SA)	0	4.38E-01	3.51E-01	3.95E-01	0.97
	1	1.73E-01	8.75E-02	1.30E-01	n/a
	2	5.57E-02	2.77E-02	4.17E-02	n/a
	3	1.80E-02	8.74E-03	1.34E-02	n/a
	4	5.80E-03	2.76E-03	4.28E-03	n/a
	5	1.87E-03	8.71E-04	1.37E-03	0.95
	6	6.04E-04	2.75E-04	4.39E-04	n/a
	7	1.95E-04	8.67E-05	1.41E-04	n/a
	8	6.29E-05	2.74E-05	4.51E-05	n/a
	9	2.03E-05	8.63E-06	1.45E-05	n/a
	10	5.34E-06	3.10E-06	4.22E-06	0.95
	20	5.37E-06	2.69E-06	4.03E-06	0.95
	25	5.35E-06	2.67E-06	4.01E-06	0.95
	30	5.34E-06	3.10E-06	4.22E-06	0.95

NUMERICAL MODELING OF RESTRICTING INTER-AQUIFER EXCHANGE

Following the model development discussed in the methodology, determination of the inter-aquifer exchange flux through the aquitard breach was performed for 0% bentonite (base model) up to 10% bentonite at 1% bentonite increments. Additionally, the % bentonite was

assumed to be applied to varying thicknesses of the UCCU upper layers at 0.5 m, 1 m, 2 m, and 5 m. A summary of hydraulic properties is provided in Table 5, extracted from Villalpando-Vizcaino et al. (2021) except for the bentonite mixture conductivities.

Table 5. Conceptual model hydraulic properties.

<table>
<tr><th></th><th>Horizontal K (m/d)</th><th>Vertical anisotropy (Kh/Kv)</th><th>Specific Storage (1/m)</th><th>Specific Yield</th><th>Remarks</th></tr>
<tr><td>Unconfined Aquifer</td><td>21.40</td><td rowspan="5">1:10 (Villalpando-Vizcaino et al., 2021)</td><td>Not applicable</td><td>0.25</td><td>Based on Villalpando-Vizcaino et al. (2021) median values.</td></tr>
<tr><td>Aquitard</td><td>$5.51x10^{-8}$</td><td>0.0014</td><td rowspan="4">Not applicable</td><td>Based on Villalpando-Vizcaino et al. (2021) minimum values.</td></tr>
<tr><td>Confined Aquifer</td><td>16.90</td><td rowspan="3">0.0033</td><td>Based on Villalpando-Vizcaino et al. (2021) median values.</td></tr>
<tr><td>Aquitard Breach</td><td>0.39</td><td>Average value obtained in the lab analysis of SA.</td></tr>
<tr><td>Breach + 10% Bentonite</td><td>$4.22x10^{-6}$</td><td>Lab values.</td></tr>
</table>

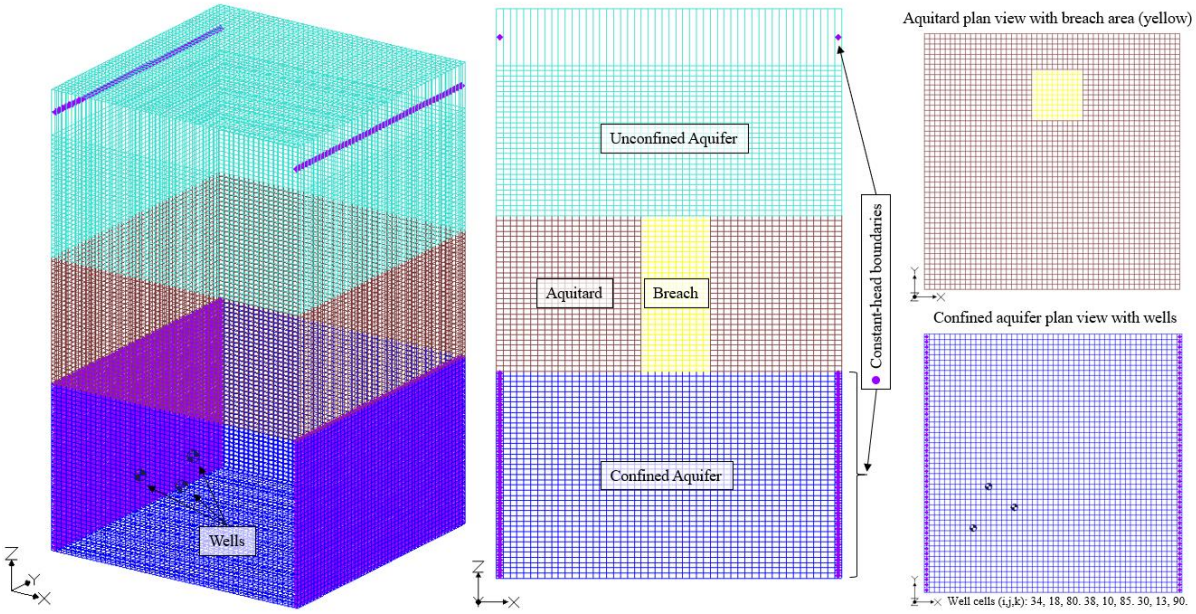

Figure 7. Multi-layer aquifer system conceptual model. Oblique view of the 3D model (left), front view showing the different units (middle), and plan views (right).

Vertical flux (q) at differing bentonite percentages is provided in Table 6. With zero bentonite added, the flux through the breach was 4.36 m/day. Non-linear reductions in q occurred for additions of bentonite as the thickness of application increased. At 6% bentonite when K_{avg} approximated the UCCU clay conductivity, the flux reduced to 0.17 m/day, then stabilized at 0.06 m/day at 9% bentonite for an applied injection thickness of 0.5 m. Using the upper flux of 0.17 m/day, equated fluxes at lower bentonite percentages occurred at thicker applications, such as using 4% bentonite applied over 5 m (vertical). Using a void ratio of 0.35 (Figure 5) and a single cell (100 m^2) the volume of bentonite at 6% at 0.5 m thick is approximately 2.5 m^3. At 4% bentonite applied over 5 m the approximate volume of bentonite is 16.2 m^3. Hence, it is more economical to use more bentonite within a smaller thickness, to obtain the same reduction in hydraulic conductivity, than to use less bentonite over larger thicknesses.

As seen in Table 5, the aquitard hydraulic conductivity (K_{aqt}) is 5.51 x 10^{-8} m/day. With no breach, the flux through the aquitard (at the breach location) was 1.65 x10^{-5} m/day. If instead K_{aqt} = 4.39 x 10^{-4} (i.e., K_{avg} at 6% (Table 4)), flux through the aquitard is 1.32 x 10^{-2} m/day which is an order of magnitude compared to the previous flux (q), .and if is replaced with K at 10% found in the lab is obtained a flux q=1.27 x 10^{-3} m/day , is still having two magnitudes of order compared to the initial flux. However, if is replaced the K_{min} from Villalpando et al. (2021), with $K_{average}$ from the same authors equal to 5.7 x 10-4 is obtained a flux q = 1.71 x 10^{-3} and compared to the fluxes from K at 6% and Kat 10% values obtained from the lab the difference in flux is one order of magnitude and same orders of magnitude, respectively. Note we used the Kat 6% and 10% average values.

Table 6. Flux with different thickness of the sand-bentonite mixture

Bentonite, %	Flux (q), m/day			
	0.5 m	1.0 m	2.0 m	5.0 m
0	4.36	4.36	4.36	4.36
1	4.10	3.87	3.48	2.67
2	3.45	2.86	2.12	1.20
3	2.31	1.57	0.96	0.44
4	1.14	0.65	0.35	0.16
5	0.44	0.24	0.14	0.08
6	0.17	0.11	0.08	0.06
7	0.09	0.08	0.07	0.06
8	0.07	0.07	0.06	0.05
9	0.06	0.06	0.06	0.05
10	0.06	0.06	0.06	0.05

It is interesting to note that if breach material is characteristic of medium to coarse sand according to Table 4, reduction of the material to mimic UCCU clay conductivities may not be possible without exceeding the optimal bentonite content (i.e., 30%) and displacing parent material with bentonite. The mechanics surrounding this shift in parent material under an overburden pressure remains to be investigated. Though this investigation did not physically

test the injection process, there does exist much information on injection methods and their effectiveness, application, and challenges (Veil & Dusseault, 2003; Namil & Gular, 2019).

CONCLUSIONS

Inter-aquifer exchange through an aquitard is a common, physical phenomenon (Clark and Hart, 2009; Villalpando et al., 2021), although the movement of groundwater through the aquitard is slow due to its characteristically low hydraulic conductivity. If not less common, then less identified, are the existence of preferential conduits in an aquitard, termed breaches, resulting from paleo-drainage erosion, faulting, or other mechanisms. Breaches offer a pathway for water of poorer quality (or contamination) to bypass the protective nature of the aquitard during heightened inter-aquifer exchange.

This study investigates the plausibility of minimizing inter-aquifer exchange via an aquitard breach by proposing injection of a bentonite slurry into the breach material to close the void space. To test this hypothesis, glass bead samples characterized as coarse, medium and fine plus a composite sand sample from an actual aquitard breach were mixed with bentonite at sequential increased percentages of solid (matrix) volume and hydraulic conductivities calculated. Comparison of experimental results with published values helped ensure that the method was producing reliable results. Following, laboratory experiments were conducted to determine hydraulic conductivities for various mixtures of glass beads and a breach sand with percentages of bentonite (0-30%). Hydraulic conductivities for coarse and medium glass beads never attained that of a local aquitard clay, the UCCU, in Shelby County, Tennessee. The bentonite percentage of 30% was considered optimal, representing a point of transition when higher percentages of bentonite replaced the glass beads. Fine glass beads closely matched the majority grain size (89%) of the breach sand; therefore, both shared the same optimal bentonite percentage of 10%. When considering the sand sample, at 6% bentonite the hydraulic conductivity of the sample resembled the UCCU clay conductivity. At 10%, the hydraulic conductivity of the sample reduces by another 2-orders of magnitude.

As conducting an injection of bentonite into a breach exceeded the scope of this investigation, a simple numerical model of a breach and inter-aquifer exchange revealed that the flux through the breach at 6% bentonite decreased from 4.36 to 0.17 m/day if applied over a thickness of 0.5 m. The flux dropped and plateaued at 0.06 m/day reaching 10% bentonite. Equivalent reductions in flux would occur for lower bentonite percentages over greater thickness but at an economic disadvantage. It was also determined that if a breach exhibited medium to coarse sand, bentonite additive to 30% would not reach hydraulic conductivities of the UCCU clay; hence, closure of the breach similar to finer sediments are not attainable. Possibly exceeding the optimal 30% for medium and coarse sediments could provide the ; however, determination of the mechanics of particle replacement when breaches are buried beneath overburden sediments remains to be studied.

Protection of drinking water aquifers, often confined beneath a confining unit such as an aquitard is of paramount interest, especially in highly urbanized areas where contamination potential is greatest. Identifying a means of breach closure whereby the preferential pathway composed of more permeable material can be reduced to a clay-like barrier offers an in-situ protection alternative. Though much must still be considered in the details of breach size, land access, depth, cost, injection methodology, and other factors, this investigation sets a reasonable precedent to further study breach closure to minimize inter-aquifer exchange.

REFERENCES

Alakayleh, Z., Clement, T., & Fang, X. (2018). Understanding the Changes in Hydraulic Conductivity Values of Coarse- and Fine-Grained Porous Media Mixtures. Water, 10. https://doi.org/10.3390/w10030313

Alkaya, D., & Esener, A. (2011). Usability of sand-bentonite-cement mixture in the construction of unpermeable layer. Scientific Research and Essays, 6. https://doi.org/10.5897/SRE10.1189

Alzamel M., Fall M., & Haruna S. (2022, March 23). Swelling ability and behavior of bentonite-based materials for deep repository engineered barrier systems: Influence of physical, chemical, and thermal factors | Elsevier Enhanced Reader. https://doi.org/10.1016/j.jrmge.2021.11.009

Anderson, E. I., & Mesa, E. (2006). The effects of vertical barrier walls on the hydraulic control of contaminated groundwater. Advances in Water Resources, 29(1), 89–98. https://doi.org/10.1016/j.advwatres.2005.05.005

ASTM. (2016). Standard Test Methods for Measurement of Hydraulic Conductivity of Saturated Porous Materials Using a Flexible Wall permeameter. https://compass.astm.org/document/?contentCode=ASTM%7CD5084-16A%7Cen-US&proxycl=https%3A%2F%2Fsecure.astm.org&fromLogin=true

Bani Baker, M., Abendeh, R., Sharo, A., & Hanna, A. (2022). Stabilization of Sandy Soils by Bentonite Clay Slurry at Laboratory Bench and Pilot Scales. Coatings, 12, 1922. https://doi.org/10.3390/coatings12121922

Bárcena, Y. A., & Hurtado, J. E. A. (1999). Ensayos de Permeabilidad en Materiales de Baja de Permeabilidad Compactados. 16.

Bradley, Mi. W. (1991). Ground-water hydrology and the effects of vertical leakage and leachate migration on ground-water quality near Shelby County Landfill, Memphis, Tennessee. https://pubs.usgs.gov/wri/wri904075/

Brom, J., Duffková, R., Haberle, J., Zajíček, A., Nedbal, V., Bernasová, T., & Křováková, K. (2021). Identification of Infiltration Features and Hydraulic Properties of Soils Based on Crop Water Stress Derived from Remotely Sensed Data. Remote Sensing, 13, 4127. https://doi.org/10.3390/rs13204127

Carmichael, J.K., Kingsbury, J.A., Larsen, Daniel, and Schoefernacker, Scott, 2018, Preliminary evaluation of the hydrogeology and groundwater quality of the Mississippi River Valley alluvial aquifer and Memphis aquifer at the Tennessee Valley Authority Allen Power Plants, Memphis, Shelby County, Tennessee: U.S. Geological Survey Open-File Report 2018–1097, 66 p., https://doi.org/10.3133/ofr20181097.

Castelbaum, D., & Shackelford, C. D. (2009). Hydraulic Conductivity of Bentonite Slurry Mixed Sands. Journal of Geotechnical and Geoenvironmental Engineering, 135(12), Article 12. https://doi.org/10.1061/(ASCE)GT.1943-5606.0000169

Chang, C. S., Wang, J. Y., & Ge, L. (2016). Maximum and minimum void ratios for sand-silt mixtures. Engineering Geology, 211, 7–18. https://doi.org/10.1016/j.enggeo.2016.06.022

Chegbeleh, L. P., Nishigaki, M., Akudago, J. A., Alim, M. A., & Komatsu, M. (2009). Laboratory Investigation of Ethanol/Bentonite Slurry Grouting into Rock Fractures: Preliminary Results. 14(1), 23–28.

Chung, C.-K., Kim, J.-H., Kim, J., & Kim, T. (2018). Hydraulic Conductivity Variation of Coarse-Fine Soil Mixture upon Mixing Ratio. Advances in Civil Engineering, 2018, 1–11. https://doi.org/10.1155/2018/6846584

Clark, B.R., and Hart, R.M., 2009, The Mississippi Embayment Regional Aquifer Study (MERAS): Documentation of a groundwater-flow model constructed to assess water availability in the Mississippi Embayment: U.S. Geological Survey Scientific Investigations Report 2009-5172, 61 p.

Cubrinovski, M., & Ishihara, K. (2002). Maximum and Minimum Void Ratio Characteristics of Sands. Soils and Foundations, 42(6), 65–78. https://doi.org/10.3208/sandf.42.6_65

Dai, G., Sheng, Y., Pan, Y., Shi, G., & Li, S. (2020). Application of a Bentonite Slurry Modified by Polyvinyl Alcohol in the Cutoff of a Landfill. Advances in Civil Engineering, 2020, e7409520. https://doi.org/10.1155/2020/7409520

Durmusoglu, E., & Corapcioglu, M. Y. (2000). Experimental Study of Horizontal Barrier Formation by Colloidal Silica. Journal of Environmental Engineering, 126(9), 833–841. https://doi.org/10.1061/(ASCE)0733-9372(2000)126:9(833)

Evans, J. C., Ruffing, D. G., Reddy, K. R., Kumar, G., & Chetri, J. K. (2020). Sustainability of Vertical Barriers for Environmental Containment. In K. R. Reddy, A. K. Agnihotri, Y. Yukselen-Aksoy, B. K. Dubey, & A. Bansal (Eds.), Sustainable Environmental Geotechnics (Vol. 89, pp. 271–283). Springer International Publishing. https://doi.org/10.1007/978-3-030-51350-4_29

Ghazi, A. F. (2015). Engineering characteristics of compacted sand-bentonite mixtures. 102.

Harbaugh, A.W. MODFLOW-2005, the U.S. Geological Survey Modular Ground-Water Model- The Ground-water Flow Process. U.S. Geological Survey Techniques and

Methods, Book 6 (A16). 2005; 253p. Available online: https://pubs.er.usgs.gov/publication/tm6A16

Holmboe, M., Wold, S., & Pettersson, T. (2011). Effects of the injection grout Silica sol on bentonite. Physics and Chemistry of the Earth, Parts A/B/C, 36, 1580–1589. https://doi.org/10.1016/j.pce.2011.07.026

Hwang, H., Yoon, J., Rugg, D., & El Mohtar, C. S. (2011). Hydraulic Conductivity of Bentonite Grouted Sand. Geo-Frontiers 2011, 1372–1381. https://doi.org/10.1061/41165(397)141

Jiménez-Martínez, J., Aravena, R., & Candela, L. (2011). The Role of Leaky Boreholes in the Contamination of a Regional Confined Aquifer. A Case Study: The Campo de Cartagena Region, Spain. Water, Air, & Soil Pollution, 215(1), 311–327. https://doi.org/10.1007/s11270-010-0480-3

Karp, J. C., Lowe, D. K., & Marusov, N. (1962). Horizontal Barriers for Controlling Water Coning. Journal of Petroleum Technology, 14(07), 783–790. https://doi.org/10.2118/153-PA

Koch, D. (2002). Bentonites as a basic material for technical base liners and site encapsulation cut-off walls. Applied Clay Science, 21(1), 1–11. https://doi.org/10.1016/S0169-1317(01)00087-4

Larsen, D., Gentry, R. W., & Solomon, D. K. (2003). The geochemistry and mixing of leakage in a semi-confined aquifer at a municipal well field, Memphis, Tennessee, USA. Applied Geochemistry, 18(7), 1043–1063. https://doi.org/10.1016/S0883-2927(02)00204-4

Lei, H., Liu, X., Shi, F., & Ma, C. (2022). Infiltration behavior into sand of bentonite slurry with guar gum. Géotechnique Letters, 12, 1–6. https://doi.org/10.1680/jgele.22.00003

Li, Q., Jia, Z., & Zhao, Y. (2021). Laboratory evaluation of hydraulic conductivity and chemical compatibility of bentonite slurry for grouting walls. Environmental Earth Sciences, 80(17), 569. https://doi.org/10.1007/s12665-021-09847-5

Li, Z., & Dou, S. (2008). Effect of bentonite on properties of injection repairing mix. 42, 133-134+138.

Li, Z., & Zhang, T. (2013). Vitrification. https://www.geoengineer.org/education/web-class-projects/cee-549-geoenvironmental-engineering-winter-2013/assignments/vitrification#recommended-reading

Ojuri, O., & Oluwatuyi, O. (2017). Strength and Hydraulic Conductivity Characteristics of Sand-Bentonite Mixtures Designed as a Landfill Liner. Jordan Journal of Civil Engineering, 11(4), 9.

Oma, K. H. (1994). In Situ Vitrification. In Hazardous Waste Site Soil Remediation. CRC Press.

Othman, B. A., & Marto, A. (2018). Laboratory test on maximum and minimum void ratio of tropical sand matrix soils. IOP Conference Series: Earth and Environmental Science, 140, 012084. https://doi.org/10.1088/1755-1315/140/1/012084

Parks, W. S. (1990). Hydrogeology and preliminary assessment of the potential for contamination of the Memphis Aquifer in the Memphis area, Tennessee /. U.S. Geological Survey.

Parks, W. S., Mirecki, J. E., & Kingsbury, J. A. (1995). Hydrogeology, Ground-water Quality, and Source of Ground Water Causing Water-quality Changes in the Davis Well Field at Memphis, Tennessee. U.S. Department of the Interior, U.S. Geological Survey.

Pearlman, L. (1999). Subsurface Barriers. https://clu-in.org/products/intern/pearlman/

Qian, H., Chen, J., & Howard, K. W. F. (2020). Assessing groundwater pollution and potential remediation processes in a multi-layer aquifer system. Environmental Pollution, 263, 114669. https://doi.org/10.1016/j.envpol.2020.114669

Riha, J., Petrula, L., Hala, M., & Alhasan, Z. (2018). Assessment of empirical formulae for determining the hydraulic conductivity of glass beads. Journal of Hydrology and Hydromechanics, 66, 337–347. https://doi.org/10.2478/johh-2018-0021

Rine, J., Shafer, J., & Covington, E. (2004). Assessing Groundwater Vulnerability and Contaminant Pathways at MCAS Beaufort, SC.

Robinson, J. L., Carmichael, J. K., Halford, K. J., & Ladd, D. E. (1997). Hydrogeologic framework and simulation of ground-water flow and travel time in the shallow aquifer system in the area of Naval Support Activity Memphis, Millington, Tennessee (Report No. 97–4228; Water-Resources Investigations Report). USGS Publications Warehouse. https://doi.org/10.3133/wri974228

Ryan, C. R. (1985). Slurry Cutoff Walls: Applications in the Control of Hazardous Wastes. https://www.astm.org/stp34562s.html

Ryan, C. R., & Day, S. R. (2002). Soil-Cement-Bentonite Slurry Walls. Deep Foundations 2002, 713–727. https://doi.org/10.1061/40601(256)51

Ryan, C., Ruffing, D., & Evans, J. (2022). Soil Bentonite Slurry Trench Cutoff Walls: History, Design, and Construction Practices. 89–99. https://doi.org/10.1061/9780784484050.010

Sakita, T., Komine, H., Yamada, A., Wang, H., & Goto, S. (2020). Influence of bentonite type and producing method on hydraulic conductivity of sand–bentonite mixture. E3S Web of Conferences, 205, 10005. https://doi.org/10.1051/e3sconf/202020510005

Sällfors, G., & Öberg-Högsta, A.-L. (2002). Determination of hydraulic conductivity of sand-bentonite mixtures for engineering purposes. Geotechnical & Geological Engineering, 20(1), 65–80. https://doi.org/10.1023/A:1013857823676

Santi, P. M., McCray, J. E., & Martens, J. L. (2006). Investigating cross-contamination of aquifers. Hydrogeology Journal, 14(1), 51–68. https://doi.org/10.1007/s10040-004-0403-8

Seki, K., Miyazaki, T., & Nakano, M. (1996). Reduction of Hydraulic Conductivity Due to Microbial Effects. Transactions of The Japanese Society of Irrigation, Drainage and Reclamation Engineering, 1996(181), 137-144,a3. https://doi.org/10.11408/jsidre1965.1996.137

Sharo, A., Khasawneh, M., Bani Baker, M., & Tarawneh, D. (2022). Sonicated waves procedure effect on stabilizing expansive soil by nano-clay: Treat with cause. Frontiers in Built Environment, 8, 975993. https://doi.org/10.3389/fbuil.2022.975993

Sivapullaiah, P. V., Sridharan, A., & Stalin, V. K. (2000). Hydraulic conductivity of bentonite-sand mixtures. Canadian Geotechnical Journal, 37(2), 406–413. https://doi.org/10.1139/t99-120

Smith, M. R. (2018). Evaluating modern recharge to the Memphis aquifer at the Lichterman well field, Memphis, Tennessee. 90.

Srikanth, V., & Mishra, A. K. (2016). A Laboratory Study on the Geotechnical Characteristics of Sand–Bentonite Mixtures and the Role of Particle Size of Sand. International Journal of Geosynthetics and Ground Engineering, 2(1), 3. https://doi.org/10.1007/s40891-015-0043-1

Staley, L. J. (1995). Vitrification Technologies for the Treatment of Contaminated Soil. In Emerging Technologies in Hazardous Waste Management V (Vol. 607, pp. 102–120). American Chemical Society. https://doi.org/10.1021/bk-1995-0607.ch009

Sun, W., Wei, Z., Sun, D., Liu, S., Fatahi, B., & Wang, X. (2015). Evaluation of the swelling characteristics of bentonite–sand mixtures. Engineering Geology, 199, 1–11. https://doi.org/10.1016/j.enggeo.2015.10.004

Syngouna, V. I., & Chrysikopoulos, C. V. (2015). Experimental investigation of virus and clay particles cotransport in partially saturated columns packed with glass beads. Journal of Colloid and Interface Science, 440, 140–150. https://doi.org/10.1016/j.jcis.2014.10.066

Takai, A., Inui, T., & Katsumi, T. (2016). Evaluating the hydraulic barrier performance of soil-bentonite cutoff walls using the piezocone penetration test. Soils and Foundations, 56(2), 277–290. https://doi.org/10.1016/j.sandf.2016.02.010

Takai, A., Inui, T., Katsumi, T., Kamon, M., & Araki, S. (2013, July 1). Hydraulic barrier performance of soil bentonite mixture cutoff wall. https://doi.org/10.1201/b15004-96

Takase, H., Iwasa, K., Ishii, T., Ueda, H., Sakabe, Y., & Ishiguro, K. (2011). Consolidation of Ethanol/Bentonite Slurry Injected in a Planar Fracture; Mathematical Modelling and Experiment. MRS Proceedings, 932. https://doi.org/10.1557/PROC-932-107.1

Tixier, J. S., & Thompson, L. E. (1993). In situ vitrification: Providing a comprehensive solution for remediation of contaminated soils (p. 15).

Trifunović, V. (2021). Vitrification as a method of soil remediation. Zaštita Materijala, 62(3), 166–179. https://doi.org/10.5937/zasmat2103166T

Veil, J. A., & Dusseault, M. B. (2003). Evaluation of slurry injection technology for management of drilling wastes. (ANL/EA/RP-109792, 819455; p. ANL/EA/RP-109792, 819455). https://doi.org/10.2172/819455

Villalpando-Vizcaino, R., Waldron, B., Larsen, D., & Schoefernacker, S. (2021). Development of a Numerical Multi-Layered Groundwater Model to Simulate Inter-Aquifer Water Exchange in Shelby County, Tennessee. Water, 13(18), Article 18. https://doi.org/10.3390/w13182583

Waldron, B., Harris, J., Larsen, D., & Pell, A. (2009). Mapping an aquitard breach using shear-wave seismic reflection. Hydrogeology Journal, 17, 505–517. https://doi.org/10.1007/s10040-008-0400-4

Wang, Q., Tang, A. M., Cui, Y.-J., Delage, P., & Gatmiri, B. (2012). Experimental study on the swelling behavior of bentonite/claystone mixture. Engineering Geology, 124, 59–66. https://doi.org/10.1016/j.enggeo.2011.10.003

Xu, H., Zhu, W., Qian, X., Wang, S., & Fan, X. (2016). Studies on hydraulic conductivity and compressibility of backfills for soil-bentonite cutoff walls. Applied Clay Science, 132–133, 326–335. https://doi.org/10.1016/j.clay.2016.06.025

Xu, T., Dias, T., & Bezuijen, A. (2017). Slurry infiltration ahead of slurry TBM's in saturated sand: Laboratory tests and consequences for practice.

Yin, K., Fauchille, A.-L., Di Filippo, E., Kotronis, P., & Sciarra, G. (2021). A Review of Sand–Clay Mixture and Soil–Structure Interface Direct Shear Test. Geotechnics, 1(2), Article 2. https://doi.org/10.3390/geotechnics1020014

Yoo, D.-J., Oh, M.-H., Kim, Y.-S., & Park, J.-B. (2006). Factors Affecting the Electrical Properties of Bentonite Slurry. Journal of the Korean Geotechnical Society, 22.

Zhang, Z., Ward, A., & Keller, J. (2009). Determining the Porosity and Saturated Hydraulic Conductivity of Binary Mixtures. 30.